

Acellular hydroxyapatite-collagen scaffolds support angiogenesis and osteogenic gene expression in an ectopic murine model: Effects of hydroxyapatite volume fraction

Matthew J. Meagher,¹ Holly E. Weiss-Bilka,¹ Margaret E. Best,¹ Joel D. Boerckel,¹ Diane R. Wagner,² Ryan K. Roeder¹

¹Department of Aerospace and Mechanical Engineering, Bioengineering Graduate Program, University of Notre Dame, Notre Dame, Indiana 46556

²Department of Mechanical Engineering, Indiana University Purdue University at Indianapolis, Indianapolis, Indiana 46202

Received 13 November 2015; revised 13 April 2016; accepted 21 April 2016

Published online 3 May 2016 in Wiley Online Library (wileyonlinelibrary.com). DOI: 10.1002/jbm.a.35760

Abstract: Acellular hydroxyapatite (HA) reinforced collagen scaffolds were previously reported to induce angiogenesis and osteogenesis after ectopic implantation but the effect of the HA volume fraction was not investigated. Therefore, the objective of this study was to investigate the effect of HA volume fraction on *in vivo* angiogenesis and osteogenesis in acellular collagen scaffolds containing 0, 20, and 40 vol % HA after subcutaneous ectopic implantation for up to 12 weeks in mice. Endogenous cell populations were able to completely and uniformly infiltrate the entire scaffold within 6 weeks independent of the HA content, but the cell density was increased in scaffolds containing HA versus collagen alone. Angiogenesis, remodeling of the original scaffold matrix, mineralization, and osteogenic gene

expression were evident in scaffolds containing HA, but were not observed in collagen scaffolds. Moreover, HA promoted a dose-dependent increase in measured vascular density, cell density, matrix deposition, and mineralization. Therefore, the results of this study suggest that HA promoted the recruitment and differentiation of endogenous cell populations to support angiogenic and osteogenic activity in collagen scaffolds after subcutaneous ectopic implantation. © 2016 Wiley Periodicals, Inc. *J Biomed Mater Res Part A*: 104A: 2178–2188, 2016.

Key Words: angiogenesis, collagen, hydroxyapatite, osteogenesis, osteoinduction, synthetic bone graft substitute, tissue engineering scaffold

How to cite this article: Meagher MJ, Weiss-Bilka HE, Best ME, Boerckel JD, Wagner DR, Roeder RK. 2016. Acellular hydroxyapatite-collagen scaffolds support angiogenesis and osteogenic gene expression in an ectopic murine model: Effects of hydroxyapatite volume fraction. *J Biomed Mater Res Part A* 2016;104A:2178–2188.

INTRODUCTION

Up to 2.2 million bone grafts are performed annually worldwide, which presents a significant clinical need for graft sources.^{1,2} The clinical gold standard is autologous bone graft which requires no processing and provides an osteoinductive graft material. However, autologous tissue is limited by graft size, shape, and complications associated with donor site morbidity which have been reported in as many as 25% of procedures.^{3–6} These complications can include donor site pain, sensory disturbances, functional disorders, and fractures.⁶ Allogeneic tissue is less constrained by availability, size, and shape, but is less osteoinductive and associated with an increased risk of immunogenic response.⁷ Therefore, limitations in autograft and allograft have led to extensive research in synthetic bone graft substitutes and bone tissue engineering scaffolds aimed at achieving the functionality of autograft and allograft while overcoming the limitations and constraints.^{1,8–10}

The important functional requirements for a synthetic bone graft substitute or scaffold are both biological and mechanical.¹¹

The scaffold should facilitate the recruitment and differentiation of progenitor cells (bioactivity), support the formation of new blood vessels (angiogenesis) within pore spaces and new bone tissue (osteogenesis) along scaffold surfaces (osteoconduction), and be gradually metabolized (bioresorption) and replaced by native tissue.¹¹ The ability to induce osteogenesis by the recruitment and osteogenic differentiation of progenitor cells (osteoinduction) is often evaluated by evidence of bone formation after implantation in an ectopic site.¹² A synthetic bone graft substitute or scaffold should also possess sufficient mechanical properties to allow surgical handling and fixation.^{8,13}

Hydroxyapatite (HA)-reinforced collagen scaffolds mimic key aspects of the composition and architecture of native bone and have been shown to be bioactive, bioresorbable, and osteoinductive.^{14,15} HA-collagen scaffolds and commercialized collagen sponges are typically prepared via lyophilization which produces high levels of porosity (80–99%) suitable for cellular infiltration and nutrient transport.^{16–21} However, lyophilized scaffolds are limited by a relatively small pore size

Correspondence to: R. K. Roeder; e-mail: rroeder@nd.edu

Contract grant sponsor: U.S. Army Medical Research and Materiel Command; contract grant number: W81XWH-09-1-0741

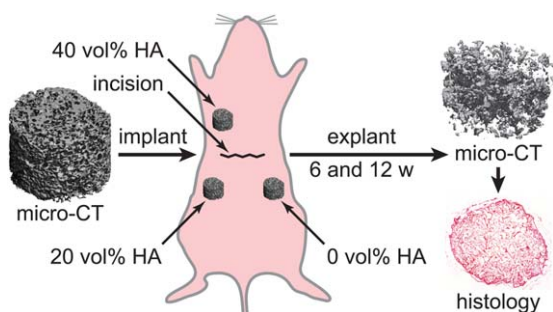


FIGURE 1. Schematic diagram showing the study design. Collagen scaffolds containing 0, 20, and 40 vol % HA were implanted within ectopic subcutaneous pockets in the dorsal cervical region of mice. Mineralization was measured by micro-CT in as-prepared scaffolds prior to implantation and at 6- or 12-weeks post-implantation. Note that the implant micro-CT image was thresholded to show the scaffold architecture in this figure while the explant image was representative of images thresholded to measure the bone volume (Fig. 2). After imaging by micro-CT, explants were also prepared for histology.

(<100 μm width) and inherently thin lamellar struts ($\sim 1\text{--}3$ μm) which result in less than ideal mechanical properties for surgical handling, fixation, and bearing osteogenic loads during healing.^{17–21}

Compression-molded HA-collagen scaffolds were recently designed to overcome the limitations of lyophilized scaffolds.^{15,22} These scaffolds were prepared with an architecture exhibiting high porosity (85–90%), spherical interconnected pores ($\sim 300\text{--}400$ μm in diameter), thicker struts ($\sim 3\text{--}100$ μm in thickness) composed of a relatively high collagen fibril density reinforced with 0–80 vol % HA, and a compressive modulus of 200–1000 kPa, which is an order of magnitude greater than lyophilized HA-collagen scaffolds.^{15,22} Scaffolds containing up to 60 vol % HA exhibited fully recoverable elastic deformation upon cyclic loading to 50% strain and were thus well-suited for surgical handling, fixation, and bearing osteogenic loads during healing.¹⁵ Moreover, there was no difference *in vitro* cellular bioactivity for scaffolds containing 40 or 80 vol % HA.¹⁵ Therefore, acellular collagen scaffolds containing 40 vol % HA were investigated *in vivo* and were observed to induce angiogenesis and osteogenesis after ectopic implantation, similar to lyophilized HA-collagen scaffolds.^{14,15} However, these previous *in vivo* studies, for both lyophilized and compression-molded HA-collagen scaffolds, did not investigate the effect of the HA volume fraction which was fixed at ~ 40 vol %.^{14,15}

Therefore, the objective of this study was to investigate the effect of HA volume fraction on *in vivo* angiogenesis and osteogenesis in acellular collagen scaffolds containing 0, 20, and 40 vol % HA after subcutaneous ectopic implantation for up to 12 weeks in mice (Fig. 1). Angiogenesis and osteogenesis were examined by micro-computed tomography (micro-CT), explant histology, and immunohistochemistry.

EXPERIMENTAL METHODS

Scaffold preparation

HA-collagen scaffolds were prepared with 85 vol % porosity and reinforced with 0, 20, or 40 vol % HA whiskers ($n = 8/\text{group}$), using previously established methods.^{15,22} Briefly, acidified type

I bovine collagen at 3.2 mg mL^{-1} (Collagen Solutions, PLC, San Jose, CA) was brought to physiological pH and ionic strength with 1 M NaOH and phosphate buffered saline (PBS). The collagen slurry was incubated at 37°C overnight to allow the solution to gel. The resulting collagen network was disrupted with a tissue homogenizer for 30 s and centrifuged at $6,000g$ for 30 min to concentrate the collagen fibrils to ~ 180 mg mL^{-1} . The concentrated collagen fibrils were collected and mixed with an appropriate amount of HA whiskers to achieve 0, 20, or 40 vol % HA within the collagen matrix of scaffolds. Single crystal, calcium-deficient HA whiskers were prepared via the chelate decomposition method under conditions previously reported to result in a mean (\pm standard deviation) length and aspect ratio of 18.0 (8.9) μm and 7.9 (3.4), respectively.^{23,24} Paraffin microspheres were then added to the HA-collagen suspension in an amount to produce scaffolds with 85% porosity. Paraffin microspheres were prepared by vigorously stirring molten paraffin into a 25 wt % solution of sucrose in water at 80°C , quickly cooling in a 2 L ice bath, and sizing with a shaker sieve to a diameter of $300\text{--}425$ μm .^{15,22}

The HA-collagen-paraffin slurry was loaded into a 6-mm diameter pellet die and compression molded at 1 MPa for 1 min such that as-pressed scaffolds exhibited a height of ~ 6 mm. Scaffolds were subsequently dried in an oven at 37°C for $24\text{--}48$ h. After drying, the paraffin porogen was leached by soaking scaffolds in successive solutions of $2 \times 100\%$ hexane (Sigma, St. Louis, MO) for 8 h, $50/50$ hexane/ethanol for 8 h, and $4 \times 100\%$ ethanol (VWR, Radnor, PA) for at least 6 h each. The volume of leaching solutions was at least $20 \times$ greater than the volume of the scaffolds. Scaffolds were subsequently crosslinked for 12 h under gentle stirring in an $80/20$ by volume solution ethanol/DI water containing 20 mM 1-ethyl-3-(3-dimethylaminopropyl)carbodiimide (EDC, Sigma) and 8 mM *n*-hydroxysuccinimide (NHS, Sigma), with pH adjusted to 7.4 using 0.1 M HCl.^{15,22}

Subcutaneous ectopic murine model

Scaffolds from each experimental group (Fig. 1) were implanted within ectopic subcutaneous pockets in the dorsal cervical region of 4-week old, female athymic nude mice (Harlan Laboratories, Indianapolis, IN) for 6 or 12 weeks ($n = 4/\text{group}/\text{time point}$). All protocols were approved by the University of Notre Dame Institutional Animal Care and Use Committee (IACUC). Scaffolds, 3 mm in diameter and height, were prepared from dehydrated scaffolds prior to porogen leaching using a biopsy punch. After porogen leaching and crosslinking, scaffolds were sterilized by soaking in 100% ethanol for 24 h, and rehydrated in sterile PBS overnight. Mice were anesthetized by intraperitoneal delivery of a cocktail containing 100 mg mL^{-1} ketamine (Henry-Schein, Dublin, OH), 20 mg mL^{-1} xylazine (Henry-Schein) and 10 mg mL^{-1} acepromazine (Henry-Schein) in sterile saline at a volumetric dose of $10 \cdot W - 50$ μL , where W is the mouse body weight (g). Scaffolds were implanted in each mouse through a small incision in the center of the dorsal region. The incision was closed with one autoclip which was removed after the wound was healed, between 7 and 10 days post-implantation. Ketoprofen (Ketofen, Henry-Schein)

was given subcutaneously at a dose of 2 mg kg⁻¹ for post-operative analgesia. Mice were sacrificed via CO₂ asphyxiation followed by cervical dislocation at 6- or 12-weeks post-implantation and scaffolds were excised for characterization.

Micro-computed tomography of scaffold implants and explants

As-prepared scaffolds were imaged by micro-CT (μ CT-80, Scanco Medical AG, Brüttisellen, Switzerland) prior to implantation and explants were imaged at 6- and 12-weeks post-implantation (Fig. 1). Both scaffold implants and explants were imaged at 10 μ m resolution, 70 kVp voltage, and 114 μ A current with 1,000 projections at 400 ms integration time with slices oriented transverse to the vertical axis of the cylindrical scaffolds. Noise in grayscale images was smoothed by Gaussian filtration with $\sigma = 0.8$ and support = 1. Mineralization was measured as the change in thresholded bone volume relative to the total volume in explants compared with as-implanted scaffolds, $\Delta(BV/TV)$, after 6- and 12-weeks implantation, in order to enable comparison between experimental groups with different levels of HA content. The bone volume (BV) was segmented from the total volume (TV) using a threshold of 212 for scaffolds containing 40 vol % HA and 196 for scaffolds containing 0 or 20 vol % HA. These thresholds were previously determined in as-prepared scaffolds by calibrating the mineral density measured by micro-CT within the segmented BV against the mineral density measured by ashing.²² Note that the thresholds of 212 and 196 corresponded to 430 and 383 mg HA cm⁻³, respectively, using a custom calibration phantom.²⁵

Histology

Explants were fixed in 4% paraformaldehyde (VWR) for 15 min, rinsed with PBS, and decalcified in 0.5M ethylenediaminetetraacetic acid (EDTA, Sigma). The EDTA solution was changed twice weekly until the addition of 1 mL of 5% sodium oxalate (Sigma) to the spent demineralization solution yielded no precipitate upon consecutive assays. Demineralized explants were equilibrated in optimal cutting temperature (OCT) compound (Tissue-Tek[®] O.C.T.[™], Sakura Finetek, Torrance, CA) for 3 h, frozen in dry ice-cooled isopentane, and stored at -80°C. Embedded explants were cryosectioned at -23°C in the coronal plane at 5–8 μ m thickness and transferred to gelatin subbed slides, which were dried at 37°C for 2 h and then stored at -80°C. Slides were warmed and dried prior to all staining procedures. Sections were warmed to room temperature and stained by hematoxylin and eosin (H&E, VWR), and modified Masson's trichrome comprising Weigert's hematoxylin (Sigma-Aldrich), xylydine ponceau (Acros Organics, Geel, Belgium), acid fuchsin (Alfa Aesar, Ward Hill, MA), phosphomolybdic acid (Tokyo Chemical Industries, Tokyo, Japan), and Fast Green FCF (Electron Microscopy Sciences, Hatfield, PA).²⁶

All sections were imaged by transmitted light microscopy (Eclipse ME600, Nikon Instruments, Melville, NY). Angiogenesis was quantified by the vascular density measured as the number of blood vessels per scaffold area (ImageJ v1.49,

National Institutes of Health). Measurements for three explants per experimental group were pooled from at least five histologic sections per explant, which were evenly spaced across the explant volume. Cell density was quantified by counting the number of nucleated cells within a 0.25 mm² region of interest (ROI) in the center of each histologic section. Matrix deposition was quantified as an area fraction in the same ROI by point counting using a 0.25 mm² grid with 81 nodes. Matrix deposition was defined as extracellular matrix deposited by infiltrating cell populations that was distinct from the scaffold matrix. Measurements for cell density and matrix deposition were pooled for three histologic sections per experimental group.

Immunohistochemistry

Immunohistochemistry was performed to detect endothelial cells associated with angiogenesis by labeling cluster of differentiation 31 (CD31), and osteogenic gene expression by labeling osteocalcin (OC) and osteopontin (OP). Antigen retrieval was performed at 80°C for 15 min in 1 mM EDTA with 0.05% Triton X-100 (Sigma-Aldrich) at pH 8.0, and blocked in 1% normal goat serum (Jackson ImmunoResearch, West Grove, PA) and 0.3M glycine (Sigma) for 4 h at 4°C. Sections were separately labeled with CD31, OC, or OP primary antibody (Abcam, Cambridge, MA) diluted to 1:200 by volume and applied in 1% bovine serum albumin (BSA, EMD Millipore, Billerica, MA) in PBS overnight at 4°C. Sections were rinsed with PBS, incubated with the fluorescent secondary antibody (AlexaFluor647 for OC and AlexaFluor 594 for OP and CD31, goat anti-rabbit, Jackson ImmunoResearch) diluted to 1:50 by volume in 1% BSA in PBS for 1 h at room temperature, counterstained with 4',6-diamidino-2-phenylindole (DAPI, Vector Laboratories, Burlington, CA) for 1 min, rinsed with PBS, and mounted in an aqueous medium. All sections were imaged by fluorescence microscopy and immunofluorescent images were overlaid on grayscale images taken by transmitted light microscopy (Nikon Eclipse ME600).

Statistical analysis

Angiogenesis (vascular density > 0) and mineralization ($\Delta(BV/TV) > 0$) were confirmed using an exact *t* test with a hypothesized mean of zero (JMP 11.0, SAS Institute, Cary, NC). Differences in $\Delta(BV/TV)$, vascular density, cellular density, and percent matrix deposition with HA content and implantation time were investigated using two-way analysis of variance (ANOVA) with a Bonferroni correction. *Post hoc* comparisons were performed using unpaired Student's *t* tests. The level of significance for all tests was set at $p < 0.05$.

RESULTS

Mineralization was measured by micro-CT as the change in thresholded bone volume relative to the total volume in explants compared with as-implanted scaffolds, $\Delta(BV/TV)$, after 6- and 12-weeks implantation (Fig. 2). Only scaffolds containing HA exhibited new mineralization ($p < 0.05$ vs. 0, exact *t* test), while scaffolds containing collagen alone did not ($p > 0.32$). Moreover, the amount of mineralization increased with increasing HA content in scaffolds ($p < 0.0001$, ANOVA).

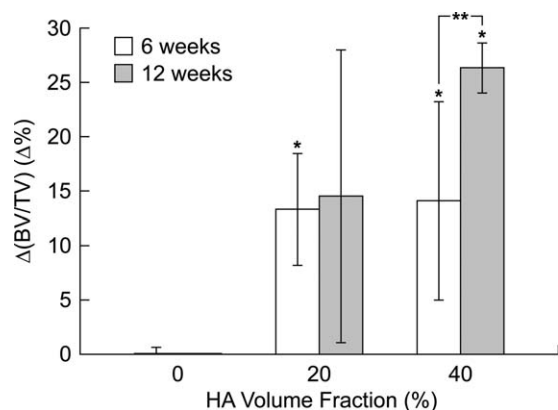


FIGURE 2. The change in thresholded bone volume relative to the total volume in explants compared with as-implanted scaffolds, $\Delta(\text{BV}/\text{TV})$, measured by micro-CT after 6- and 12-weeks implantation for scaffolds containing 0, 20, and 40 vol % HA. * $p < 0.05$ vs. $\Delta(\text{BV}/\text{TV}) = 0$, exact t test. ** $p < 0.05$, 6 vs. 12 weeks, t test.

Scaffolds containing 40 vol % HA exhibited a further increase in mineralization between 6- and 12-weeks post-implantation ($p < 0.05$, t test) while scaffolds containing 20 vol % HA did not ($p > 0.45$).

After 6-weeks implantation, stained histologic sections from explants revealed uniform cellular infiltration throughout the entire pore volume of scaffolds (Fig. 3), and that the original scaffold architecture (gray arrows) was still apparent (Fig. 4), regardless of the HA content. Collagen scaffolds exhibited relatively low cell density and no angiogenesis (Figs. 3 and 4). In contrast, collagen scaffolds containing HA exhibited increased cell density and matrix deposition (white arrows) with increased HA content (Fig. 3). Importantly, angiogenesis (black arrows) appeared to be more widespread in scaffolds with 40 vol % HA compared with 20 vol % HA (Figs. 3 and 4).

After 12-weeks implantation, stained histologic sections from explants revealed increased cell density and matrix deposition (white arrows) with increased HA content (Fig. 3). All or most of the original scaffold architecture (gray arrows) remained apparent in scaffolds containing 0 or 20 vol % HA, respectively (Fig. 4). Angiogenesis and matrix deposition were not observed in collagen scaffolds but were evident in scaffolds with 20 vol % HA (Figs. 3 and 4). In contrast, scaffolds with 40 vol % HA exhibited widespread angiogenesis (black arrows), matrix deposition (white arrows), and extensive remodeling such that none of the original scaffold architecture remained. Vascularized scaffolds or vascularized regions of scaffolds maintained healthy cell populations, while non-vascularized scaffolds or regions of scaffolds exhibited decreased cell density compared with 6 weeks regardless of the HA content (Figs. 3 and 4).

Angiogenesis was quantified from H&E stained histologic sections (Fig. 3) as the vascular density measured by the number of blood vessels per scaffold area after 6- and 12-weeks implantation [Fig. 5(a)]. Only scaffolds containing HA exhibited angiogenesis ($p < 0.05$ vs. 0 mm^{-2} , exact t test), while scaffolds containing collagen alone did not ($p > 0.21$). Moreover, the vascular density increased with increasing HA content in scaffolds

($p < 0.0001$, ANOVA), but pairwise differences between scaffolds with 20 and 40 vol % HA ($p > 0.07$, t test), and between 6- and 12-weeks post-implantation ($p = 0.07$, ANOVA), were not statistically significant.

Cellular infiltration was quantified from trichrome stained histologic sections (Fig. 4) as the cell density measured by the number of nucleated cells per scaffold area after 6- and 12-weeks implantation for scaffolds containing 0, 20, and 40 vol % HA [Fig. 5(b)]. Cellular infiltration was observed in all scaffolds ($p < 0.05$ vs. 0 mm^{-2} , exact t test). The cell density increased with increasing HA content in scaffolds ($p < 0.0001$, ANOVA) and was increased for scaffolds containing HA compared with collagen alone ($p < 0.05$ vs. 0 vol % HA, t test) for all groups except 20 vol % HA at 12-weeks post-implantation. The cell density was decreased with time ($p < 0.0001$, ANOVA) and pairwise differences were statistically significant for scaffolds containing HA ($p < 0.05$, t test), but not collagen alone ($p > 0.15$, t test).

Matrix deposition was quantified from trichrome stained histologic sections (Fig. 4) as the percent area fraction after 6- and 12-weeks implantation for scaffolds containing 0, 20, and 40 vol % HA [Fig. 5(c)]. Matrix deposition was observed in all scaffolds ($p < 0.05$ vs. 0%, exact t -test). Matrix deposition increased with increasing HA content in scaffolds ($p < 0.0001$, ANOVA) and was increased for scaffolds containing HA compared with collagen alone ($p < 0.05$ vs. 0 vol % HA, t test) for all groups except 20 vol % HA at 6-weeks post-implantation. Matrix deposition was increased with time ($p < 0.001$, ANOVA) and all pairwise differences were statistically significant ($p \leq 0.05$, t test).

Immunohistochemistry was used to confirm the presence of endothelial cells associated with angiogenesis by immunolabeling for CD31 (green) and osteogenic gene expression by immunolabeling for OC (red) and OP (green). Infiltrating mouse cells were counterstained by DAPI (blue). Collagen scaffolds did not exhibit positive staining for CD31, OC, and OP at either 6 or 12 weeks after implantation, and the cell density decreased between 6 and 12 weeks (Fig. 6, insets). Scaffolds containing 40 vol % HA exhibited positive staining for CD31, which was colocalized with cell populations but diffuse after 6-weeks implantation and became stronger and more localized by 12 weeks (Fig. 6). Positive staining for CD31 was also correlated with cell and tissue morphologies indicative of vasculature in the explants. Scaffolds containing 40 vol % HA also exhibited positive staining for OC or OP, which were colocalized with cell populations but diffuse after 6-weeks implantation (Fig. 6). After 12-weeks implantation, positive staining for cell populations and either OC or OP became much stronger and less colocalized. OC and OP were instead localized to regions of significant matrix deposition which became depopulated by cells between 6 and 12 weeks.

DISCUSSION

Acellular collagen scaffolds containing 0, 20, and 40 vol % HA were implanted within subcutaneous ectopic pockets in mice for up to 12 weeks to investigate the effects of the HA

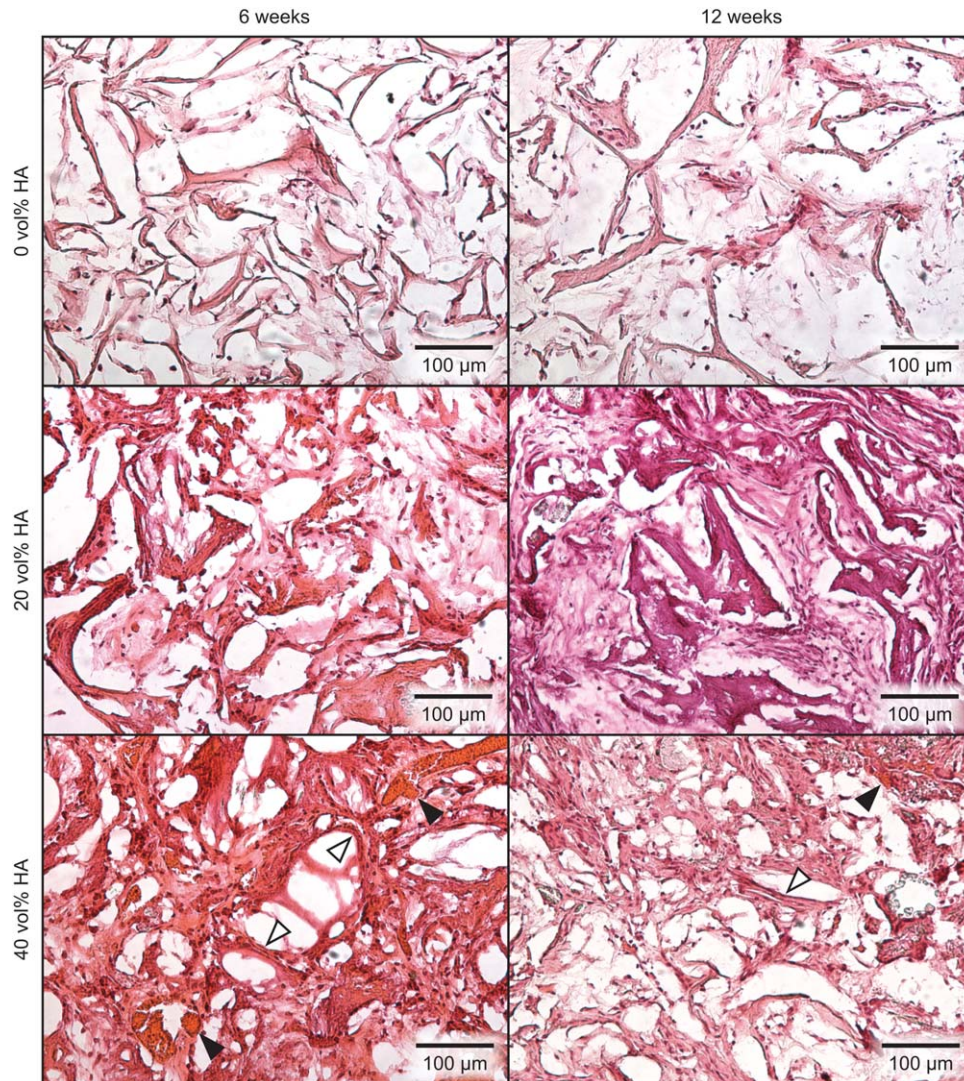


FIGURE 3. Representative H&E stained histological sections from explants after 6- and 12-weeks implantation for collagen scaffolds containing 0, 20, and 40 vol % HA. After 6-weeks implantation, uniform cellular infiltration was evident throughout the entire pore volume regardless of the HA content. Collagen scaffolds exhibited relatively low cell density and no angiogenesis at either time point. In contrast, collagen scaffolds containing HA exhibited increased cell density and matrix deposition (white arrows) with increased HA content. Importantly, scaffolds with 40 vol % HA also exhibited widespread angiogenesis (black arrows), but scaffolds with 20 vol % HA did not. After 12-weeks implantation, scaffolds with 40 vol % HA exhibited matrix deposition (white arrows), as the architecture appeared to be rearranged by infiltrating cells.

volume fraction on angiogenesis and osteogenesis. Collagen scaffolds (0 vol % HA) exhibited the lowest cell density, no angiogenesis, no matrix deposition, no remodeling of the original scaffold matrix, no mineralization, and no osteogenic gene expression. Collagen scaffolds containing 20 vol % HA exhibited increased cell density, angiogenesis, matrix deposition, remodeling of the original scaffold matrix, and mineralization, but most of the original scaffold matrix remained at 12 weeks and there was no further increase in mineralization between 6 and 12 weeks. Collagen scaffolds containing 40 vol % HA exhibited a further increase in cell density, widespread angiogenesis, matrix deposition, extensive remodeling such that none of the original scaffold matrix remained at 12 weeks, mineralization which continued to increase between 6 and 12 weeks, and osteogenic

gene expression. These differences were observed even though endogenous cell populations were able to completely and uniformly infiltrate the entire scaffold within 6 weeks regardless of the HA content, and the scaffold architecture was not significantly altered by the HA content.¹⁵ Therefore, the results of this study suggest that the HA volume fraction provided differences in chemotactic signaling to endogenous cell populations.

Osteogenesis

Acellular collagen scaffolds containing ~40 vol % HA prepared by lyophilization¹⁴ or compression-molding,¹⁵ were previously reported to be osteogenic after intramuscular and subcutaneous ectopic implantation, respectively, but the effect of the HA volume fraction was not investigated. In this study,

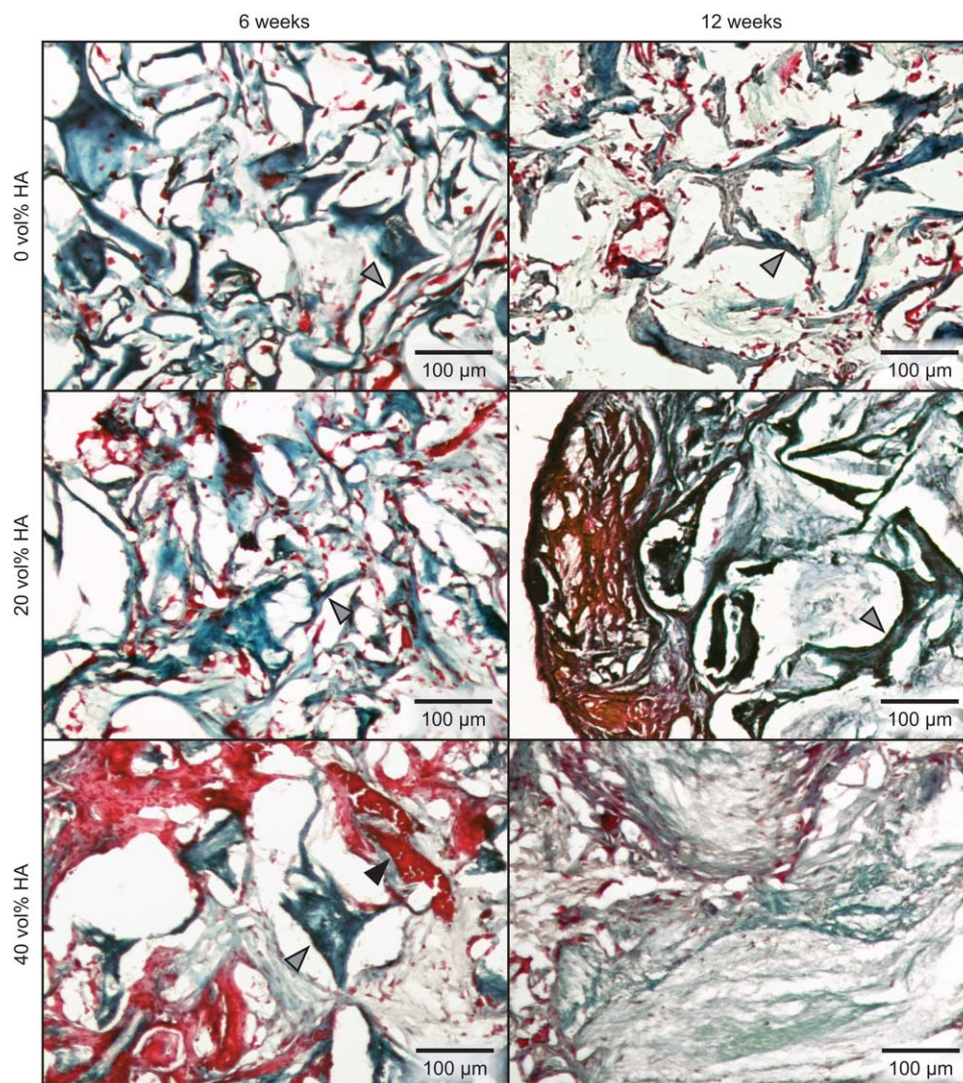


FIGURE 4. Representative Masson's trichrome stained histological sections from explants after 6- and 12-weeks implantation for collagen scaffolds containing 0, 20, and 40 vol % HA. After 6-weeks implantation, uniform cellular infiltration was evident throughout the entire pore volume, and the original scaffold architecture (gray arrows) was still apparent, regardless of the HA content. Collagen scaffolds exhibited relatively low cell density and no angiogenesis at either time point. In contrast, collagen scaffolds containing HA exhibited increased cell density with increased HA content. Scaffolds with 40 vol % HA also exhibited angiogenesis (black arrows), but scaffolds with 20 vol % HA did not. After 12-weeks implantation, all or most of the original scaffold architecture (gray arrows) remained apparent in scaffolds containing 0 or 20 vol % HA, respectively. In contrast, scaffolds with 40 vol % HA exhibited extensive remodeling such that none of the original scaffold architecture remained.

HA was shown to promote osteogenic cell differentiation, gene expression, and mineralization in acellular collagen scaffolds that otherwise exhibited no evidence of osteogenic activity after subcutaneous ectopic implantation (Figs. 2 and 6). HA was also shown to promote a dose-dependent increase in measured cell density, matrix deposition, and mineralization (Fig. 2 and 5).

Subcutaneous ectopic implantation is advantageous for investigating the osteogenic potential of scaffolds, or osteoinduction, because the subdermal microenvironment contains a low number of endogenous bone-forming cells and thus provides a more challenging microenvironment compared with intramuscular models.^{12,27} Moreover, murine models have been reported to have a lower osteoinductive potential com-

pared to larger animals.^{28,29} These and other observations have led researchers to conclude that osteoinduction is most fundamentally defined by the recruitment and osteogenic differentiation of endogenous progenitor cells.^{30,31} Therefore, observations in this study of the recruitment and osteogenic differentiation of endogenous cell populations after subcutaneous ectopic implantation in mice suggest that the HA-collagen scaffolds were osteoinductive.

The infiltration and osteogenic differentiation of endogenous progenitor cells in HA-collagen scaffolds was evidenced by increased cell density and matrix deposition, respectively (Figs. 3–5), and upregulated osteogenic gene expression (Fig. 6), with increased HA content. Previous *in vitro* investigations have typically reported no difference in cell proliferation

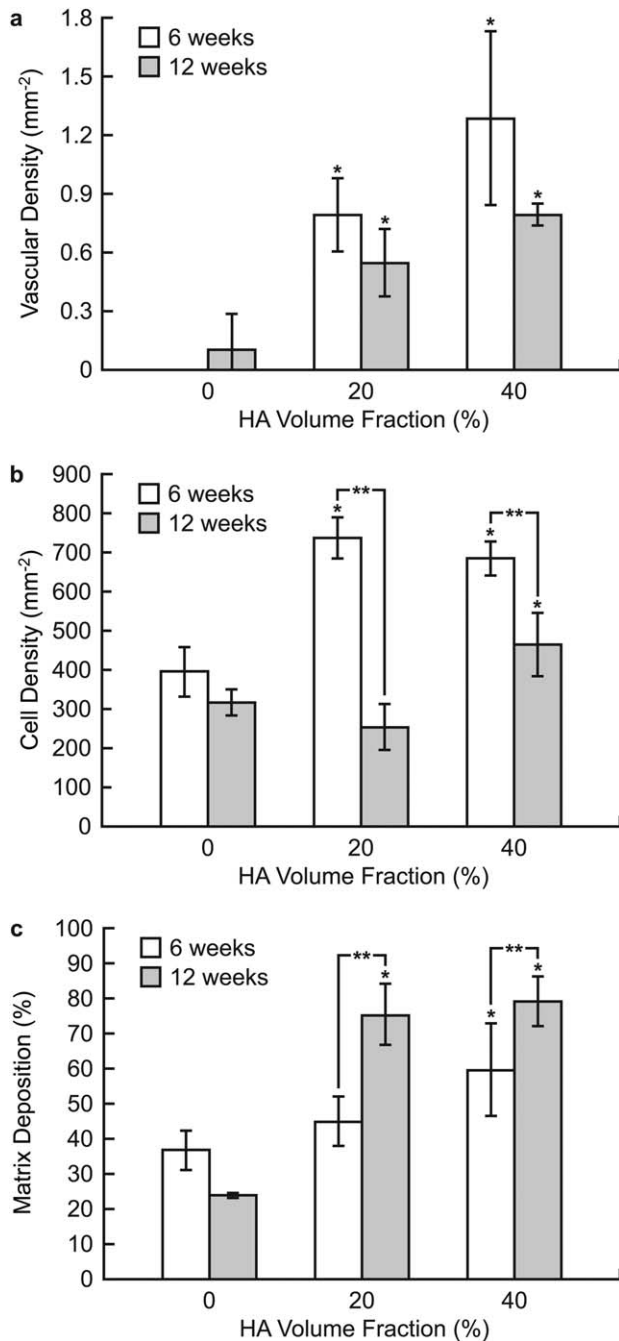


FIGURE 5. (a) Angiogenesis measured from H&E stained histologic sections (Fig. 3) as the vascular density after 6- and 12-weeks implantation for scaffolds containing 0, 20, and 40 vol % HA. * $p < 0.05$ vs. 0 mm⁻², exact t test, and vs. 0 vol % HA, t test. Cellular infiltration and matrix deposition measured from trichrome stained histologic sections (Fig. 4) as the (b) cell density, and (c) percent matrix deposition, after 6- and 12-weeks implantation for scaffolds containing 0, 20, and 40 vol % HA. * $p < 0.05$ vs. 0 vol % HA, t test. ** $p \leq 0.05$, 6 vs. 12 weeks, t test.

between lyophilized collagen and HA-collagen scaffolds for up to 21 days in cell culture after seeding with either primary osteoblasts or osteoprogenitor cells.^{14,19,32,33} In a previous study using identical scaffolds to those in the present study, murine adipose-derived stromal cells (mASCs) exhibited lower

proliferation, as measured by total DNA, and greater differentiation, as measured by alkaline phosphatase (ALP) activity, on HA-collagen scaffolds compared with collagen scaffolds after 7 and 14 days in cell culture.¹⁵ Differences between scaffolds containing 40 and 80 vol % HA were not statistically significant.¹⁵ However, ALP activity was previously shown to be greater for primary osteoblasts cultured on polymer substrates containing 40 vol % HA compared with 20 vol % HA after 7–14 days.³⁴ Therefore, the increase in cell density observed in scaffolds with increased HA content was most likely due to HA promoting greater recruitment of osteoprogenitor cells to scaffolds rather than greater proliferation of cells that infiltrated scaffolds. Moreover, osteogenic differentiation of progenitor cells that infiltrated HA-collagen scaffolds was due to the well-known bioactivity of HA.^{15,20,35}

The mechanism by which HA promotes the recruitment and differentiation of osteoprogenitor cells is not yet fully understood but key factors have been identified.^{27,36} Various calcium phosphates have been reported to be osteoinductive after subcutaneous ectopic implantation^{27,28,31,36–39} of biomaterials that typically contain both macro- and micro-porosity.²⁷ Hypothesized mechanisms include chemotactic signaling to cells by (1) the adsorption of endogenous growth factors (e.g., bone morphogenetic proteins) to calcium phosphates, (2) the release of calcium ions from calcium phosphates, and, interestingly, (3) cell signaling even in the absence of (1) and (2).^{27,30,36} Macro-porosity facilitates cell, protein, and nutrient transport, while both macro- and micro-porosity provide high surface area for the adsorption of proteins⁴⁰ and/or release of calcium ions.²⁷ Therefore, increased HA content in collagen scaffolds may have facilitated greater adsorption of endogenous growth factors, greater release of calcium ions, and/or greater osteogenic gene expression, which provided greater chemotactic signals to endogenous cell populations.

Angiogenesis

HA also promoted angiogenesis in collagen scaffolds that otherwise exhibited no angiogenesis [Figs. (2 and 5)(a), and 6]. Moreover, the angiogenicity of HA-collagen scaffolds was greater in scaffolds containing 40 vol % HA compared with 20 vol % HA. Previous studies demonstrated angiogenesis after intramuscular implantation of acellular HA scaffolds,^{41,42} and subcutaneous ectopic implantation of acellular HA-collagen scaffolds^{15,43} and bioglass-coated collagen scaffolds,⁴⁴ but the effects of HA volume fraction were less clear. A study investigating the effect of up to ~0.5 vol % HA reported no effect after 1-week implantation,⁴³ but our results suggest that as much as 20 vol % HA and 6 weeks were required to observe an effect [Fig. 5(a)]. Subcutaneous ectopic implantation is advantageous for investigating the angiogenic potential of scaffolds because the subdermal microenvironment contains limited native vasculature and thus provides a more challenging microenvironment compared with intramuscular models because endothelial cells must be recruited from adjacent tissue.^{12,45} Therefore, the results of this study suggest that HA-collagen scaffolds promoted the recruitment of endogenous endothelial cells.

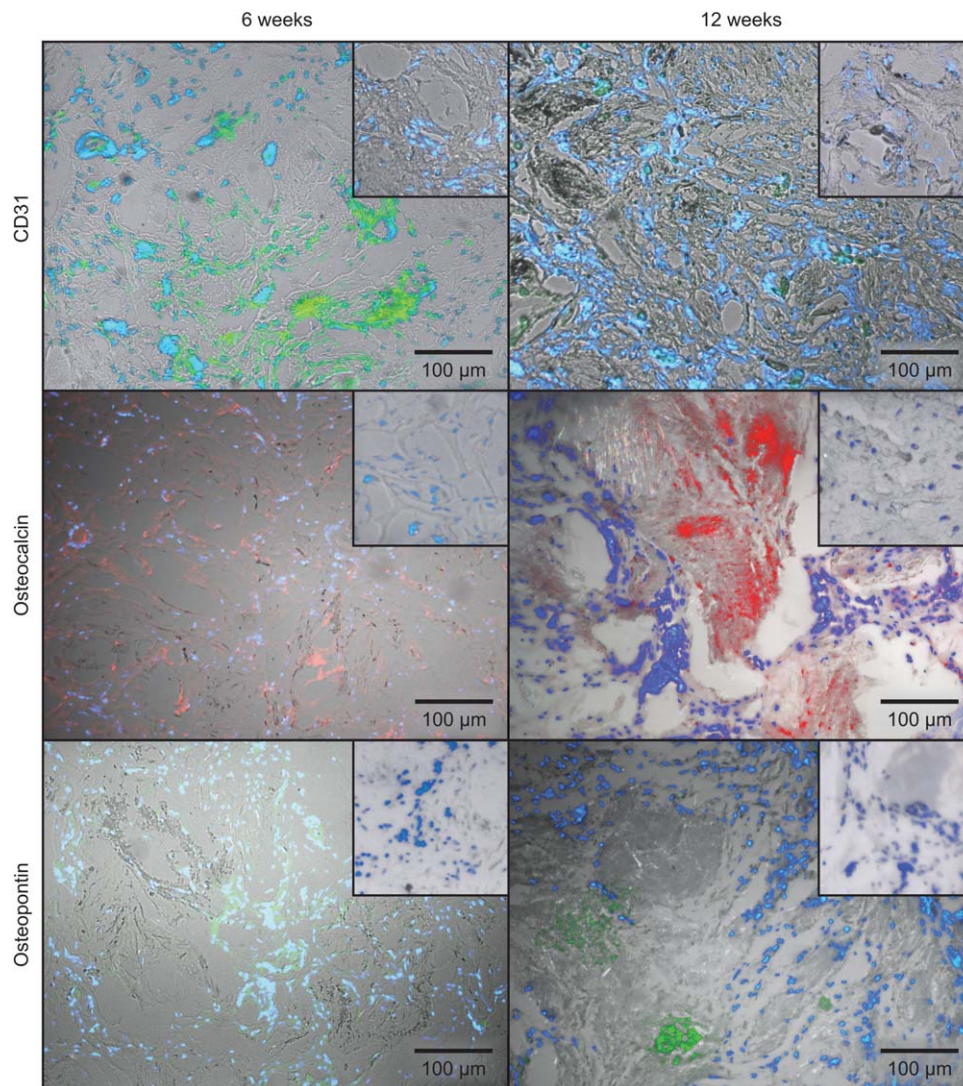


FIGURE 6. Representative histologic sections from explants after 6- and 12-week implantation for collagen scaffolds containing 0 (inset) and 40 vol % HA showing immunostaining for a marker of angiogenesis, cluster of differentiation 31 (green, CD31), markers of osteogenesis, including osteocalcin (red, OC) or osteopontin (green, OP), and counterstaining of infiltrating mouse cells (blue, DAPI), overlaid on grayscale images. Collagen scaffolds containing 40 vol % HA exhibited positive staining for CD31, OC, and OP, which was colocalized with cell populations but diffuse after 6-weeks implantation, and became stronger 12 weeks. Positive staining for CD31 became more localized by 12 weeks; OC and OP were less colocalized by 12 weeks but were instead localized to regions of significant matrix deposition which became depopulated by cells between 6 and 12 weeks. In contrast, collagen scaffolds did not exhibit positive staining for CD31, OC, or OP at either 6 or 12 weeks (insets).

There are several mechanisms by which HA could promote angiogenesis via recruitment of endothelial cells. Bioglass research has suggested that the release of calcium ions upon dissolution provides chemotactic signals which may stimulate fibroblasts to secrete angiogenic growth factors (e.g., vascular endothelial growth factor) and/or recruit endothelial cells.⁴⁶ HA may also promote the adsorption of endogenous angiogenic growth factors. Finally, scaffold or matrix stiffness may also govern angiogenesis, as described in greater detail below.

Angiogenesis is essential for functional bone regeneration via either intramembranous or endochondral ossification.^{47–49} Vascularization promotes oxygen tension, nutrient delivery, waste removal, osteoblastogenesis, and bone formation.^{48–50} Moreover, vascularization may promote the delivery

of osteoprogenitor cells to defect sites even in the absence of periosteal and marrow-derived osteoprogenitor cells,⁵¹ and is necessary to push the fate of progenitor cells away from a chondrogenic lineage and toward an osteogenic lineage.^{52,53} Thus, for all these reasons, the ability of HA-collagen scaffolds to promote angiogenesis without exogenous angiogenic growth factors or cell populations is promising for bone regeneration, but further evaluation is necessary in preclinical models for orthotopic defects.

Remodeling

The results of this study suggest that HA also promoted remodeling of collagen scaffolds that otherwise exhibited no remodeling. Granulation tissue that was observed histologically in HA-collagen scaffold explants provides a dynamic

source of active progenitor cell populations which may have induced reorganization and phagocytosis of the scaffold material.⁵⁴ Collagen scaffold explants did not exhibit granulation tissue (Fig. 3). Moreover, as discussed below, collagen scaffolds were also prone to cell-mediated contraction resulting in pore collapse (Fig. 3) due to a lower stiffness compared with HA-collagen scaffolds.¹⁵ Finally, histology did not reveal the presence of any multinucleated cells suggestive of osteoclast activity. However the release of OP by osteoblasts (Fig. 6) signals the activation of osteoclasts and the beginning of remodeling.⁵⁵

Biomechanical considerations

Differences in the HA content of scaffolds in this study may have presented differences in mechanical signals in addition to chemotactic signals. The mean (\pm standard deviation) compressive modulus of collagen scaffolds reinforced with 0, 20, and 40 vol % HA whiskers was previously reported as 100 (8), 330 (25), and 525 (58) kPa, respectively.¹⁵ Thus, HA reinforcement produced a five-fold increase in the compressive modulus. These differences in mechanical properties may have contributed to the results of this study in two important ways.

First, the collagen scaffolds were previously shown to exhibit contraction and peripheral pore collapse after *in vitro* cell culture, but HA-collagen scaffolds did not.¹⁵ Therefore, cell infiltration, angiogenesis, and nutrient transport may have been restricted in the collagen scaffolds due to peripheral pore collapse long before the 6-week time point. In contrast, HA-collagen scaffolds were able to resist the contractile forces applied by cells and maintain an open pore network at the scaffold periphery.

Second, the stiffness of a cell substrate is well-known to modulate cell phenotype.⁵⁶ Thus, the increased stiffness of scaffolds with increased HA content may have contributed to the recruitment and differentiation of osteoprogenitor cells in addition the chemotactic effects described above. Several studies have demonstrated a significant effect of scaffold stiffness on endothelial tube formation *in vitro*.^{57–60} These studies have hypothesized that cellular contraction of a relatively compliant scaffold matrix induces remodeling and disrupts endothelial tube formation. The increased matrix stiffness due to HA reinforcement prevents scaffold contraction,¹⁵ and may therefore promote endothelial tube formation. There is, however, presently a lack of consensus as other studies reported that increased matrix stiffness opposes endothelial tube formation and capillary invasion.^{61,62}

Functional significance

HA-collagen scaffolds were shown to provide advantageous chemotactic and/or biomechanical signals compared to collagen scaffolds. Moreover, acellular HA-collagen scaffolds were able to promote angiogenesis, mineralization, and osteogenic gene expression without delivering exogenous cells or growth factors. Therefore, the results of this study suggest that these scaffolds may have clinical utility as a synthetic bone graft substitute or tissue engineering scaffold

that directs endogenous cell populations, or as a delivery vehicle for exogenous growth factors and/or osteogenic cell populations which may hasten bone regeneration. In either case, future studies are required to investigate functional outcomes in critical-size orthotopic defect models.

CONCLUSIONS

Subcutaneous ectopic implantation of acellular collagen scaffolds containing 0, 20, and 40 vol % HA for up to 12 weeks in mice revealed differences in the signals provided to endogenous cell populations for directing angiogenesis and osteogenesis. Scaffolds containing HA exhibited angiogenesis, remodeling of the original scaffold matrix, mineralization, and osteogenic gene expression, while scaffolds containing collagen alone did not. Moreover, HA promoted a dose-dependent increase in measured vascular density, cell density, matrix deposition, and mineralization. Therefore, HA promoted the recruitment and differentiation of endogenous cell populations to support angiogenic and osteogenic activity in collagen scaffolds after subcutaneous ectopic implantation.

ACKNOWLEDGMENTS

The authors acknowledge the Freimann Life Science Center at the University of Notre Dame for the care of animals.

REFERENCES

1. Zimmermann G, Moghaddam A. Allograft bone matrix versus synthetic bone graft substitutes. *Injury* 2011;42: S16–S21.
2. Lewandowski KU, Gresser JD, Wise DL, Trantol DJ. Bioresorbable bone graft substitutes of different osteoconductivities: A histologic evaluation of osteointegration of poly(propylene glycol-co-fumaric acid)-based cement implants in rats. *Biomaterials* 2000; 21:757–764.
3. Giannoudis PV, Calori GM, Begue T, Schmidmaier G. Bone regeneration strategies: Current trends but what the future holds? *Injury* 2013;44::S1–S2.
4. Schaaf H, Lendeckel S, Howaldt H-P, Streckbein P. Donor site morbidity after bone harvesting from the anterior iliac crest. *Oral Surg Oral Med Oral Pathol Oral Radiol Endod* 2010;109:52–58.
5. Dimitriou R, Mataliotakis GI, Angoules AG, Kanakaris NK, Giannoudis PV. Complications following autologous bone graft harvesting from the iliac crest and using the RIA: A systematic review. *Injury* 2011;42: S3–S15.
6. Kim DH, Rhim R, Li L, Martha J, Swaim BH, Banco RJ, Jennis LG, Tromanhauser SG. Prospective study of iliac crest bone graft harvest site pain and morbidity. *Spine J* 2009;9:886–892.
7. Greenwald AS, Boden SD, Goldberg VM, Khan Y, Laurencin CT, Rosier RN. Bone-graft substitutes: Facts, fictions, and applications. *J Bone Joint Surg Am* 2001;83-A:98–103.
8. O'Brien FJ. Biomaterials and scaffolds for tissue engineering. *Mater Today* 2011;14:88–95.
9. Salgado AJ, Coutinho OP, Reis RL. Bone tissue engineering: State of the art and future trends. *Macromol Biosci* 2004;4:743–765.
10. Szpalski C, Wetterau M, Barr J, Warren SM. Bone tissue engineering: Current strategies and techniques—Part I: Scaffolds. *Tissue Eng Part B Rev* 2012;18:246–257.
11. Calori GM, Mazza E, Colombo M, Ripamonti C. The use of bone-graft substitutes in large bone defects: Any specific needs? *Injury* 2011;42: S56–S63.
12. Scott MA, Levi B, Askarinam A, Nguyen A, Rackohn T, Ting K, Soo C, James AW. Brief review of models of ectopic bone formation. *Stem Cells Dev* 2012;21:655–667.
13. Giannoudis PV, Chris Arts JJ, Schmidmaier G, Larsson S. What should be the characteristics of the ideal bone graft substitute? *Injury* 2011;42: S1–S2.

14. Murphy CM, Schindeler A, Gleeson JP, Yu NYC, Cantrill LC, Mikulec K, Peacock L, Little DG. A collagen-hydroxyapatite scaffold allows for binding and co-delivery of recombinant bone morphogenetic proteins and bisphosphonates. *Acta Biomater* 2014; 10:2250–2258.
15. Kane RJ, Weiss-Bilka HE, Meagher MJ, Liu Y, Gargac JA, Niebur GL, Wagner DL, Roeder RK. Hydroxyapatite reinforced collagen scaffolds with improved architecture and mechanical properties. *Acta Biomater* 2015;17:16–25.
16. Geiger M, Li RH, Friess W. Collagen sponges for bone regeneration with rhBMP-2. *Adv Drug Deliv Rev* 2003;55:1613–1629.
17. Harley BA, Leung JH, Silva ECCM, Gibson LJ. Mechanical characterization of collagen-glycosaminoglycan scaffolds. *Acta Biomater* 2007;3:463–474.
18. Tierney CM, Haugh MG, Liedl J, Mulcahy F, Hayes B, O'Brien FJ. The effects of collagen concentration and crosslink density on the biological, structural and mechanical properties of collagen-GAG scaffolds for bone tissue engineering. *J Mech Behav Biomed Mater* 2009;2:202–209.
19. Cunniffe GM, Dickson GR, Partap S, Stanton KT, O'Brien FJ. Development and characterisation of a collagen nano-hydroxyapatite composite scaffold for bone tissue engineering. *J Mater Sci Mater Med* 2010;21:2293–2298.
20. Gleeson JP, Plunkett NA, O'Brien FJ. Addition of hydroxyapatite improves stiffness, interconnectivity and osteogenic potential of a highly porous collagen-based scaffold for bone tissue engineering. *Eur Cells Mater* 2010;20:218–230.
21. Kane RJ, Roeder RK. Effects of hydroxyapatite reinforcement on the architecture and mechanical properties of freeze-dried collagen scaffolds. *J Mech Behav Biomed Mater* 2012;7:41–49.
22. Meagher MJ, Kane RJ, Curtis TE, Best ME, Weiss-Bilka HE, Wagner DR, Roeder RK. Fabrication methods for hydroxyapatite reinforced collagen scaffolds with tailored architecture and improved functionality. JOM, submitted.
23. Roeder RK, Converse GL, Leng H, Yue W. Kinetic effects on hydroxyapatite whiskers synthesized by the chelate decomposition method. *J Am Ceram Soc* 2006;89:20962104.
24. Roeder RK, Sproul MS, Turner CH. Hydroxyapatite whiskers provide improved mechanical properties in reinforced polymer composites. *J Biomed Mater Res* 2003;67A:801–812.
25. Deuerling JM, Rudy DJ, Niebur GL, Roeder RK. Improved accuracy of cortical bone mineralization measured by polychromatic microcomputed tomography using a novel high mineral density composite calibration phantom. *Med Phys* 2010;37:5138–5145.
26. Jennings B, Farquhar M, Moon H. Staining methods for osmium-methacrylate sections. *Am J Pathol* 1959;35:991–997.
27. Habibovic P, De Groot K. Osteoinductive biomaterials—Properties and relevance in bone repair. *J Tissue Eng Regen Med* 2007;1:25–32.
28. Barradas AMC, Yuan H, van der Stok J, Le Quang B, Fernandes H, Chaterjea A, Hogenes MCH, Shultz K, Donahue LR, Blitterswijk C, de Boer J. The influence of genetic factors on the osteoinductive potential of calcium phosphate ceramics in mice. *Biomaterials* 2012;33:5696–5705.
29. Wang L, Zhang B, Bao C, Habibovic P, Hu J, Zhang X. Ectopic osteoid and bone formation by three calcium-phosphate ceramics in rats, rabbits and dogs. *PLoS One* 2014;9:e107044.
30. Lin L, Chow KL, Leng Y. Study of hydroxyapatite osteoinductivity with an osteogenic differentiation of mesenchymal stem cells. *J Biomed Mater Res* 2009;89A:326–335.
31. Miron RJ, Zhang YF. Osteoinduction: A review of old concepts with new standards. *J Dental Res* 2012;91:736–744.
32. Liu L, Zhang L, Ren B, Wang F, Zhang Q. Preparation and characterization of collagen-hydroxyapatite composite used for bone tissue engineering scaffold. *Artif Cells Blood Substit Biotechnol* 2003;31:435–448.
33. Jones GL, Walton R, Czernuszka J, Griffiths SL, Haj El AJ, Cartmell SH. Primary human osteoblast culture on 3D porous collagen-hydroxyapatite scaffolds. *J Biomed Mater Res* 2010;94A:1244–1250.
34. Di Silvio L, Dalby MJ, Bonfield W. Osteoblast behaviour on HAP/PE composite surfaces with different HA volumes. *Biomaterials* 2002;23:101–107.
35. Shu R, McMullen R, Baumann MJ, McCabe LR. Hydroxyapatite accelerates differentiation and suppresses growth of MC3T3-E1 osteoblasts. *J Biomed Mater Res* 2003;67A:1196–1204.
36. LeGeros RZ. Properties of osteoconductive biomaterials: Calcium phosphates. *Clin Orthop Rel Res* 2002; 81–98.
37. Gosain AK, Song L, Riordan P, Amarante MT, Nagy PG, Wilson CR, Toth JM, Ricci JL. A 1-year study of osteoinduction in hydroxyapatite-derived biomaterials in an adult sheep model: Part I. *Plast Reconstr Surg* 2002;109:619–630.
38. Le Nihouannen D, Daculsi G, Saffarzadeh A, Gauthier O, Delplace S, Pilet P, Layrolle P. Ectopic bone formation by microporous calcium phosphate ceramic particles in sheep muscles. *Bone* 2005; 36:1086–1093.
39. Yuan H, van Blitterwijk CA, de Groot K, de Bruijn JD. Cross-species comparison of ectopic bone formation in biphasic calcium phosphate (BCP) and hydroxyapatite (HA) scaffolds. *Tissue Eng* 2006;12:1607–1615.
40. Rouahi M, Gallet O, Champion E, Dentzer J, Hardouin P, Anselme K. Influence of hydroxyapatite microstructure on human bone cell response. *J Biomed Mater Res* 2006;78A:222–235.
41. Rucker M, Laschke MW, Junker D, Carvalho C, Tavassol F, Mülhaupt R, Gellrich N, Menger MD. Vascularization and biocompatibility of scaffolds consisting of different calcium phosphate compounds. *J Biomed Mater Res* 2008;86A:1002–1011.
42. Wang H, Zhi W, Lu X, Li X, Duan K, Duan R, Mu Y, Weng J. Comparative studies on ectopic bone formation in porous hydroxyapatite scaffolds with complementary pore structures. *Acta Biomater* 2013;9:8413–8421.
43. Rao RR, Ceccarelli J, Vigen ML, Gudur M, Singh R, Deng CX, Putnam AJ, Stegemann JP. Effects of hydroxyapatite on endothelial network formation in collagen/fibrin composite hydrogels *in vitro* and *in vivo*. *Acta Biomater* 2014;10:3091–3097.
44. Andrade AL, Andrade SP, Domingues RZ. *In vivo* performance of a sol-gel glass-coated collagen. *J Biomed Mater Res* 2006;79B: 122–128.
45. Wise JK, Sumner DR, Viridi AS. Modulation of stromal cell-derived factor-1/CXC chemokine receptor 4 axis enhances rhBMP-2-induced ectopic bone formation. *Tissue Eng A* 2012;18:860–869.
46. Gorustovich AA, Roether JA, Boccaccini AR. Effect of bioactive glasses on angiogenesis: A review of *in vitro* and *in vivo* evidences. *Tissue Eng B* 2009;16:199–207.
47. Hausman MR, Schaffler MB, Majeska RJ. Prevention of fracture healing in rats by an inhibitor of angiogenesis. *Bone* 2001;29:560–564.
48. Kanczler JM, Oreffo ROC. Osteogenesis and angiogenesis: The potential for engineering bone. *Eur Cells Mater* 2008;15:100–114.
49. Hankenson KD, Dishowitz M, Gray C, Schenker M. Angiogenesis in bone regeneration. *Injury* 2011;42:556–561.
50. Boerckel JD, Uhrig BA, Willett NJ, Huebsch N, Guldberg RE. Mechanical regulation of vascular growth and tissue regeneration *in vivo*. *Proc Natl Acad Sci USA* 2011;108:E674–680.
51. Collett GDM, Canfield AE. Angiogenesis and pericytes in the initiation of ectopic calcification. *Circ Res* 2005;96:930–938.
52. Deckers MML, van Bezooijen RL, van der Horst G, Hoogendam J, van der Bent C, Papapoulos SE, Löwik CWGM. Bone morphogenetic proteins stimulate angiogenesis through osteoblast-derived vascular endothelial growth factor A. *Endocrinology* 2002;143: 1545–1553.
53. Kakudo N, Kusumoto K, Wang YB, Iguchi Y, Ogawa Y. Immunolocalization of vascular endothelial growth factor on intramuscular ectopic osteoinduction by bone morphogenetic protein-2. *Life Sci* 2006;79:1847–1855.
54. Yokoyama A, Gelinsky M, Kawasaki T, Kohgo T, König U, Pompe W, Watari F. Biomimetic porous scaffolds with high elasticity made from mineralized collagen—An animal study. *J Biomed Mater Res* 2005;75B:464–472.
55. Reinholt FP, Hulthén K, Oldberg A, Heinegård D. Osteopontin—A possible anchor of osteoclasts to bone. *Proc Natl Acad Sci USA* 1990;87:4473–4475.
56. Engler AJ, Sen S, Sweeney HL, Discher DE. Matrix elasticity directs stem cell lineage specification. *Cell* 2006;126:677–689.
57. Rao RR, Peterson AW, Ceccarelli J, Putnam AJ, Stegemann JP. Matrix composition regulates three-dimensional network

- formation by endothelial cells and mesenchymal stem cells in collagen/fibrin materials. *Angiogenesis* 2012;15:253–264.
58. Mason BN, Starchenko A, Williams RM, Bonassar LJ, Reinhart-King CA. Tuning three-dimensional collagen matrix stiffness independently of collagen concentration modulates endothelial cell behavior. *Acta Biomater* 2013;9:4635–4647.
 59. Lee PF, Bai Y, Smith RL, Bayless KJ, Yeh AT. Angiogenic responses are enhanced in mechanically and microscopically characterized, microbial transglutaminase crosslinked collagen matrices with increased stiffness. *Acta Biomater* 2013;9:7178–7190.
 60. Sieminski AL, Hebbel RP, Gooch KJ. The relative magnitudes of endothelial force generation and matrix stiffness modulate capillary morphogenesis *in vitro*. *Exp Cell Res* 2004;297:574–584.
 61. Critser PJ, Kreger ST, Voytik-Harbin SL, Yoder MC. Collagen matrix physical properties modulate endothelial colony forming cell-derived vessels *in vivo*. *Microvasc Res* 2010;80:23–30.